A Novel FET Model Including an Illumination-Intensity Parameter for Simulation of Optically Controlled Millimeter-Wave Oscillators

Shigeo Kawasaki, Hidehisa Shiomi, and Kazuoki Matsugatani

***Abstract*—This paper demonstrates an illuminated FET model including an illumination-intensity parameter for simulation of optical characteristics of microwave and millimeter wave integrated circuits (MMIC's). Modeling for an illuminated GaAs MESFET and an InP high electron-mobility transistor (HEMT), and analysis and experimental results from optically controlled microwave and millimeter-wave hybrid integrated circuit (HIC) and MMIC oscillators are discussed. The proposed illuminated FET model was able to explain the photoresponse of both the GaAs MESFET and the InP HEMT, and the photooperation of their circuits.**

I. Introduction

RECENT developments in microwave and millimeter-wave technologies and in optoelectronic technologies have allowed multimedia network systems consisting of a wireless communication system and an optical-fiber communication system to be realized. In accordance with this fact, in microwave photonics, millimeter-wave signal distribution through the optical fiber is of growing interest [1]. In this system, the millimeter-wave signal in the fiber can travel for a long distance as if in free space, hence, the variety of the application possibility for the optical-fiber communication system increases [2]. In order to realize this system with multifunctions, small size, light weight, low cost, and high efficient conversion between light waves and millimeter waves is desired [3]. Among various technologies, the monolithic microwave integrated circuit (MMIC) utilizing the light wave and the radio wave interaction (i.e., the photonic MMIC) is one of the promising candidates to achieve these requirements [4].

In the photonic MMIC, the characteristics change due to interaction between the light-wave and the semiconductor device [5]. For instance, the MMIC oscillator, which is directly illuminated by a continuous and/or pulsed optical signal, can be controlled, injection locked, modulated, and converted when the radio waves are carried by the optical signal through the optical fiber. In recent research work [6], [7], illuminated microwave transistors such as MESFET's, high electron-mobility transistors (HEMT's), or heterojunction bipolar transistors (HBT's) have been used as a low-cost and simple photodetector [8]. This operation mainly results from the photovoltaic and photoconductive effects of these transistors.

When the photonic MMIC is designed in such a way as to involve the optical phenomena mentioned above, the circuit designer is immediately aware of the necessity of a good model including a parameter for the optical illumination intensity. For this purpose, an illuminated FET model has been proposed for the self-aligned MESFET by some of the authors [9]. This proposed model worked well for the investigation of the microwave characteristics of the photonic HMIC oscillator under illumination in the simulation.

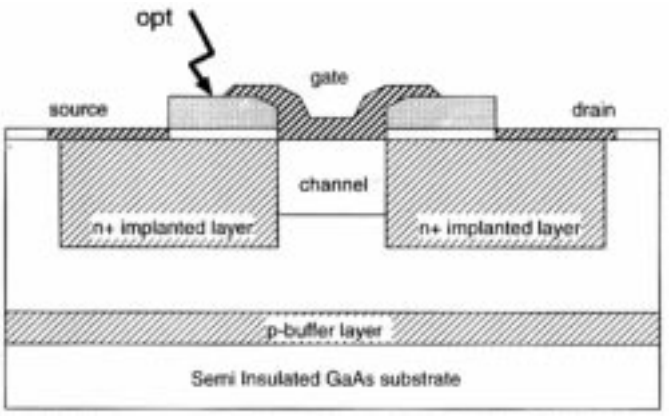

Fig. 1. MESFET structure.

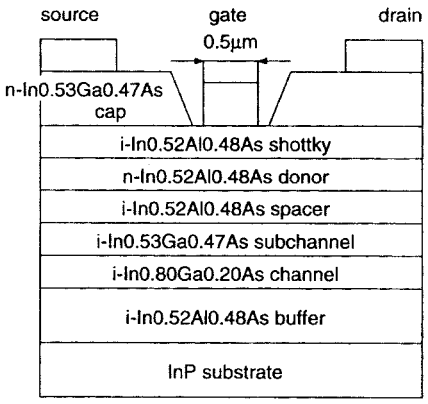

Fig. 2. HEMT structure.

Manuscript received October 15, 1997; revised March 4, 1998. This work was supported in part by the research support funds of the Dean of the School of Engineering, Tokai University, and the grants of the Telecommunication Frontier Research and Development, the Ministry of Post and Telecommunication, Japan.

S. Kawasaki and H. Shiomi are with the Department of Communications Engineering, Tokai University, Hiratsuka, Kanagawa 259-12, Japan (e-mail: kawasaki@keyaki.cc.u-tokai.ac.jp).

K. Matsugatani is with the DENSO Corporation, Research Laboratory, Aichi 470-01, Japan.

Publisher Item Identifier S 0018-9480(98)04070-8.

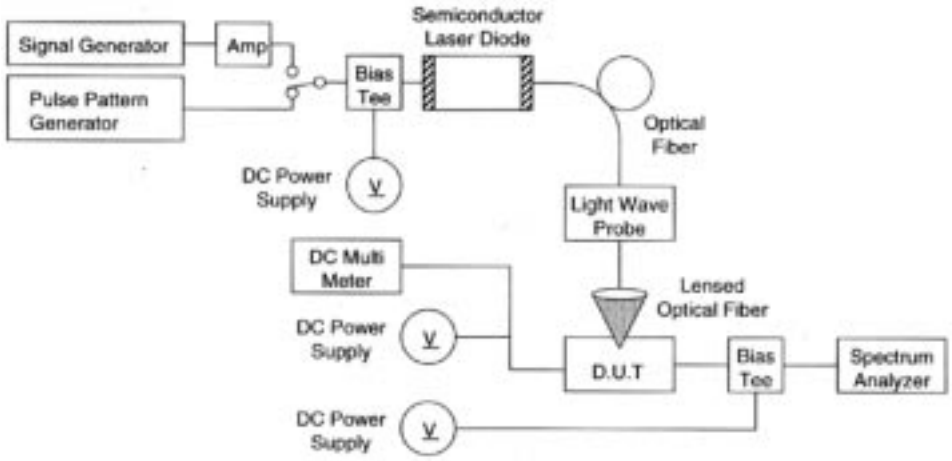

Fig. 3. Experimental setup for MESFET.

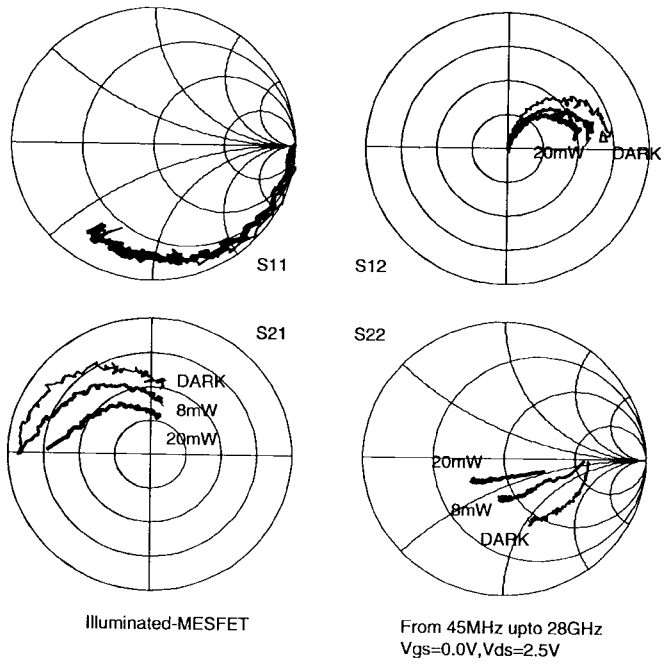

(a)

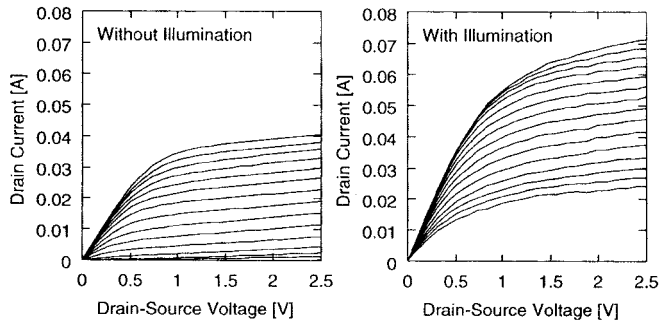

(b)

Fig. 4. Measured dc and RF characteristics of MESFET.

In this paper, for the general nonlinear FET simulation, the illuminated MESFET model is extended to an InP HEMT with the illumination intensity parameter interacting with the FET model parameters. In addition, nonlinear analysis of the device and design of an optically controlled oscillator using the proposed illuminated FET model are described. Although the photoresponse of the FET depends on the wavelength of the illumination source, the proposed illuminated FET model works well in both cases. Comparison of the experimental data from the fabricated optically controlled hybrid microwave integrated circuit (HMIC) and MMIC oscillators with the calculated ones are also considered in this paper.

II. Device Characteristics

In order to establish an accurate FET model including optical parameters, a preliminary experiment of the dc characteristic and the S-parameter measurement were carried out for both FET's. Structures of a self-aligned GaAs MESFET and an InP HEMT are indicated in Figs. 1 and 2. The MESFET used had a 0.15-μm-long 100-μm-wide gate and the HEMT had a gate length of 0.5 μm and a gatewidth of 52 μm.

Direct optical illumination was carried out from the top of the FET. Throughout the aperture (between the metal electrodes), an optical signal intruded into the FET. The optical source for the MESFET was a semiconductor laser ($\lambda = 820$ nm, maximum output power $= 20$ mW) where its output was guided to an illuminated point on the MESFET by a multimode optical fiber with a spherical lens. A laser-spot diameter was about 10 μm. The experimental setup for the MESFET is shown in Fig. 3. The other source for the HEMT was a semiconductor laser ($\lambda = 635$ nm, maximum output power $= 1$ mW) and its output was focused on the HEMT by the lens. The spot diameter in this case was about 8 mm.

The measured dc characteristics and the small-signal S-parameters from both the MESFET and the HEMT are indicated in Figs. 4 and 5, respectively. In both cases, the drain current increased due to the illumination, and the apparent difference resulting from illumination effect were observed in the S-parameter measurement.

III. FET Modeling

Utilizing the measured data obtained above, establishment of the illuminated FET model was carried out. For this purpose, using a typical small-signal FET model, Y-parameters

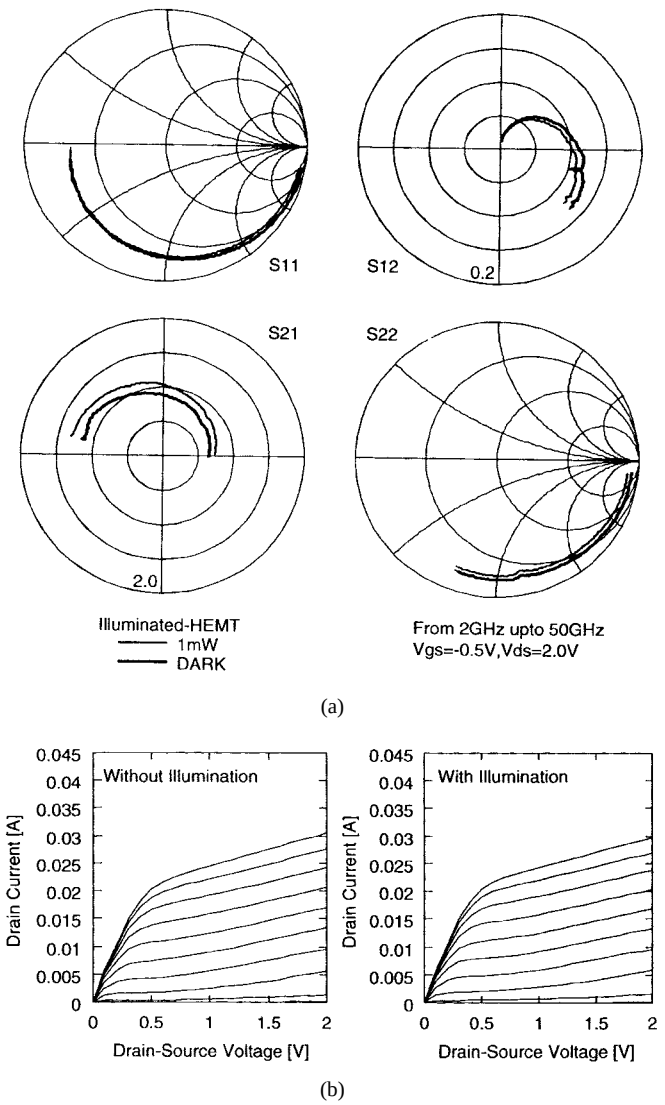

Fig. 5. Measured dc and RF characteristics of HEMT.

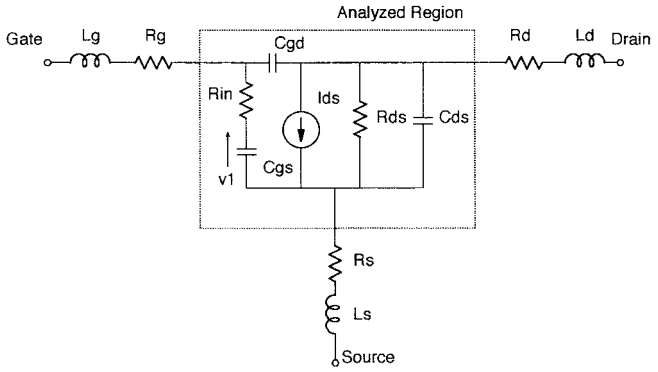

Fig. 6. Typical FET model.

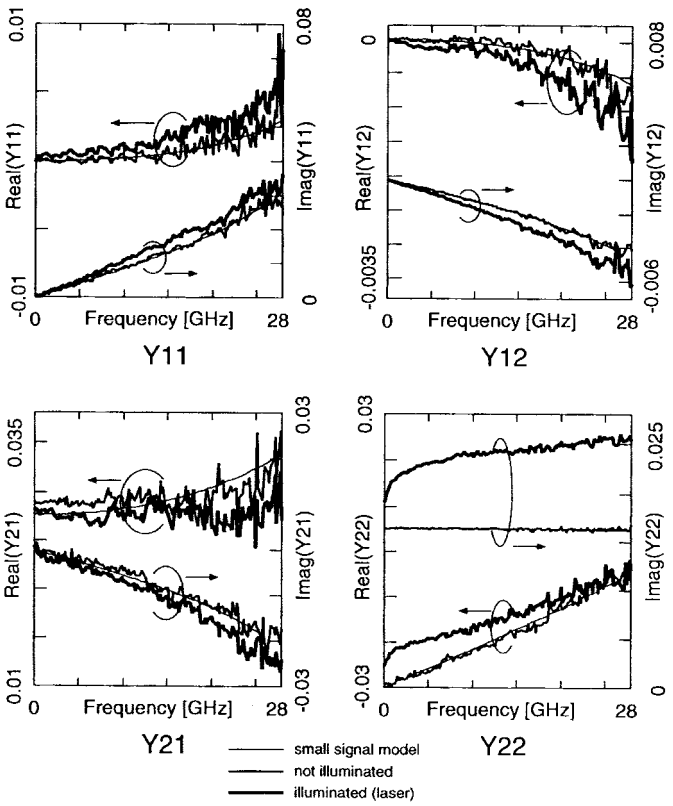

Fig. 7. Y-parameter comparison for MESFET.

were investigated within the analyzed region, as shown in Fig. 6. From the measured data, the processed Y-parameters for the analyzed region are indicated in Figs. 7 and 8 for the MESFET and the HEMT, respectively. The equations of the Y-parameters for the analyzed region of the typical model indicated in Fig. 6 are

$$y_{11} = \frac{\omega^2 C_{\rm gs}^2 R_{\rm in}}{1+(\omega C_{\rm gs} R_{\rm in})^2} + j\omega\left\{\frac{C_{\rm gs}}{1+(\omega C_{\rm gs} R_{\rm in})^2} + C_{\rm dg}\right\} \quad (1)$$

$$y_{12} = -j\omega C_{\rm dg} \quad (2)$$

$$y_{21} = \frac{g_m}{1+(\omega C_{\rm gs} R_{\rm in})^2} - j\omega\left\{\frac{C_{\rm gs} R_{\rm in} g_m}{1+(\omega C_{\rm gs} R_{\rm in})^2} + C_{\rm dg}\right\} \quad (3)$$

$$y_{22} = \frac{1}{R_{\rm ds}} + j\omega(C_{\rm dg} + C_{\rm ds}). \quad (4)$$

The extracted model parameters shown in Fig. 6 are indicated in Table I. In addition, in order to make clear comparison between the experimental data and the theoretical curves, computed curves using the typical FET model (shown in Fig. 6) formulated in (1)–(4) were also indicated in Figs. 7 and 8. Please note that the model in Fig. 6 is the small-signal model and can be compared with the experimental data under the "dark" condition only.

From these observations, significant differences can be seen on the real part of y_{22} in the MESFET and the real part of y_{21} and y_{22} in the HEMT. By taking these facts into account, a novel FET equivalent-circuit model for both FET's was established, and is shown in Fig. 9. The extracted model parameters using the model shown in Fig. 9 are indicated in Table II. A photoresponse of the HEMT epilayer seems to be the same as the case of the MESFET, since the laser energy with 635 nm is almost absorbed in each epilayer. Since the InP HEMT structure is not well known, a profile for the band diagram and the electron carrier intensity is indicated in Fig. 10. It seems that the photogenerated carriers can be created in the depletion layer, the channel layer and the InAlAs layer, which are indicated in Fig. 2 as well as in Fig. 10.

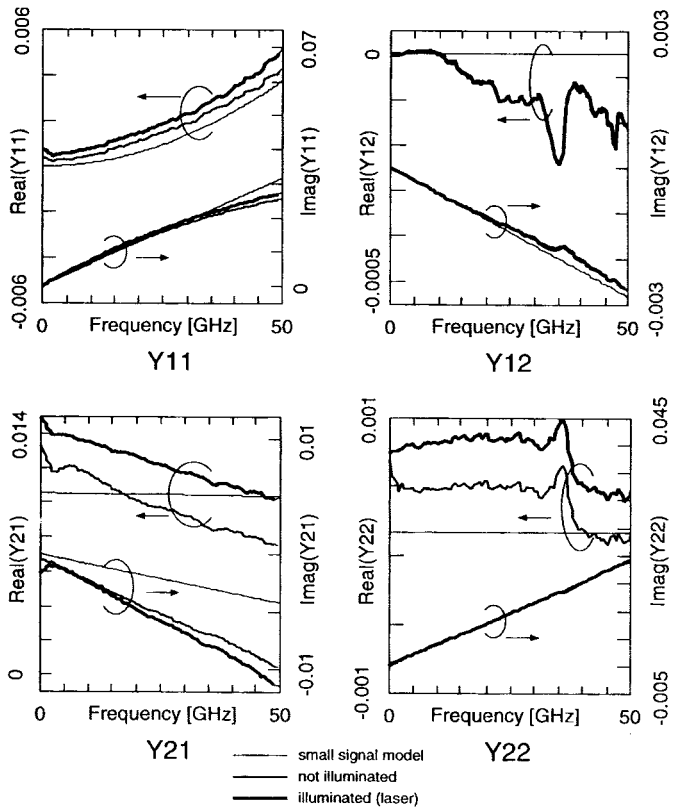

Fig. 8. Y-parameter comparison for HEMT.

TABLE I
COMPONENT PARAMETERS OF THE TYPICAL FET MODEL

MESFET under dark condition		HEMT under dark condition	
Circuit Parameter	Extracted Value	Circuit Parameter	Extracted Value
gm	29.2 ms	gm	10.5 ms
Rds	210 Ω	Rds	5.9k Ω
Cgs	103 fF	Cgs	94.2 fF
Cgd	18.7 fF	Cgd	9.01 fF
Cds	42.7 fF	Cds	52.4 fF
Rin	1.00 Ω	Rin	4.46 Ω
Rg	3.00 Ω	Rg	1.00 Ω
Rd	6.37 Ω	Rd	1.91 Ω
Rs	0.10 Ω	Rs	0.10 Ω
Lg	66.4 pH	Lg	0.11 nH
Ld	3.55 pH	Ld	0.05 nH
Ls	1.00 fH	Ls	0.10 nH

From the comparison between the proposed model described above and the device structure seen in Figs. 1 and 2, it should be noted that, from the illumination resistance $R_{\rm opt}$ and the illumination capacitance $C_{\rm opt}$ in the MESFET model, the current flow occurs in the substrate region due to reduction of the barrier height by the internal photovoltaic effect, as introduced in [6]. In the case of the HEMT, though the thickness of the absorbing layer was small, the same phenomenon seems to occur, since all layers can absorb the light energy with the wavelength of 635 nm.

From the view point of application to the telecommunication, careful attention should be paid for selection of the wavelength of the optical source, since the wavelength determines which layer with the specified energy band gap

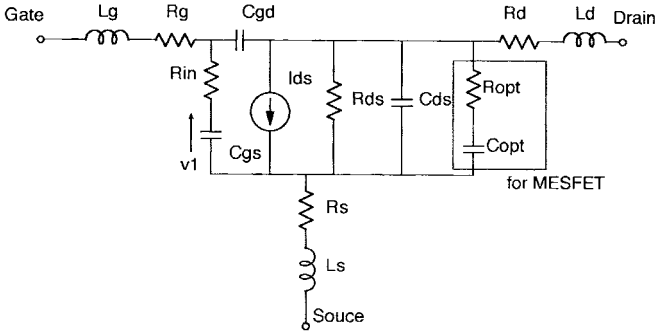

Fig. 9. Illuminated FET model.

TABLE II
COMPONENT PARAMETERS OF THE ILLUMINATED FET MODEL

MESFET under illumination of 20mW		HEMT under illumination of 1mW	
Circuit Parameter	Extracted Value	Circuit Parameter	Extracted Value
gm	32.5 ms	gm	12.9 ms
Rds	210 Ω	Rds	1.7k Ω
Cgs	111 fF	Cgs	100 fF
Cgd	27.5 fF	Cgd	8.69 fF
Cds	105 fF	Cds	52.4 fF
Rin	1.00 Ω	Rin	4.46 Ω
Rg	3.00 Ω	Rg	1.00 Ω
Rd	6.37 Ω	Rd	1.91 Ω
Rs	0.10 Ω	Rs	0.10 Ω
Lg	66.4 pH	Lg	0.11 nH
Ld	3.55 pH	Ld	0.05 nH
Ls	1.00 fH	Ls	0.10 nH
Copt	15.3 pF	Copt	1.00 fF
Ropt	53.5 Ω	Ropt	1MΩ
α	3.30	α	5.88
β	0.0288	β	0.0338
γ	0.111	γ	0.0195
Aopt	0.00107	Aopt	1E-5
$\alpha_{\rm opt}$	1.71	$\alpha_{\rm opt}$	10
V_{T00}	-1.01	V_{T00}	-0.509

can generate photocarriers. In this paper, in order to observe the photoresponse of the device using the small laser power clearly, the wavelength of the laser diode was selected from the relatively short wavelength region. In other words, the selected and photoresponsable epilayer should be grown in the device for the sake of the special application such as 1.5 μm for the telecommunication.

By using the novel model, illumination intensity dependence of each model parameter was appreciated by means of parameter extraction from measured S-parameters and from $I_{\rm ds}$ to $V_{\rm ds}$ characteristic curves with and without illumination. For the basic small-signal model and the nonlinear elements in the model, the Golio's model [10] and the modified Statz model [11] were used. Formulation for the nonlinear drain current for both FET's is

$$I_{\rm ds} = \frac{\beta(V_{\rm gs}-V_T)^Q(1+\lambda V_{\rm ds})}{1+b(V_{\rm gs}-V_T)} \tanh(\alpha V_{\rm ds}) + I_{\rm opt} \quad (5)$$

and

$$I_{\rm opt} = A_{\rm opt} \times P_{\rm opt}(1+\lambda V_{\rm ds}) \tanh(\alpha_{\rm opt} V_{\rm ds})$$

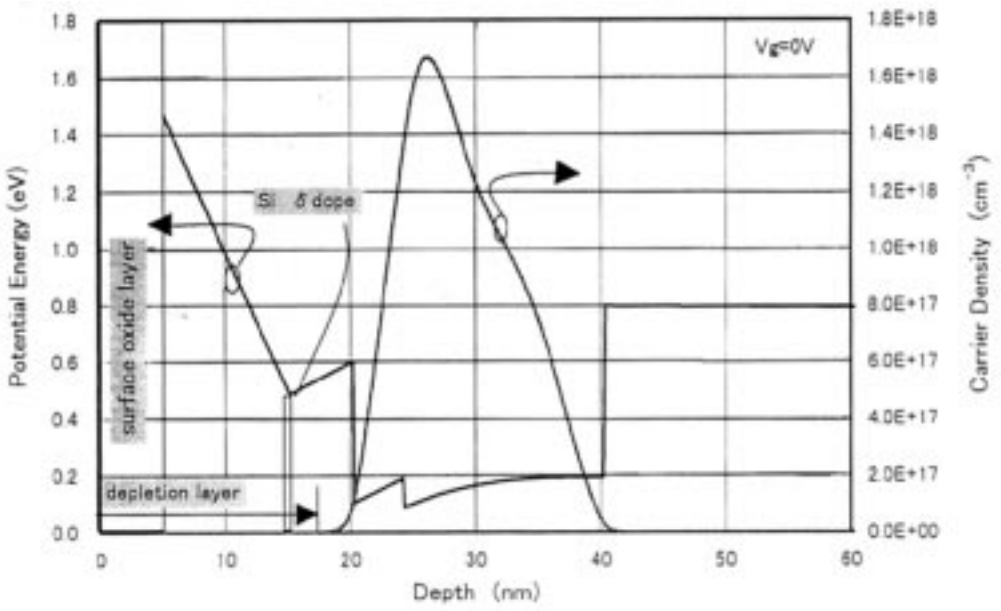

Fig. 10. Band diagram and carrier intensity.

where Q is constant due to $V_{\rm gs}$ dependence and $A_{\rm opt}$ and $\alpha_{\rm opt}$ are constants due to the illumination. The other coefficients are

$$\begin{aligned}
\alpha &= \frac{\alpha_1}{1+\alpha_2\dfrac{V_{\rm gs}}{-V_{T0}}} \\
V_T &= V_{T0}-\gamma V_{\rm ds} \\
V_{T0} &= V_{T00}\,\frac{(V_{T01}P_{\rm opt}+V_{T02})}{(V_{T02}P_{\rm opt})} \qquad (6)\\
C_{\rm gs} &= \frac{C_{\rm gs0}\times C_{\rm gs_opt}}{\left(1-\dfrac{V_{\rm new}}{V_{bi}}\right)^{U}}\times K_0\times K_1\times C_{\rm gd0}\times C_{\rm gd_opt}\times K_2 \\
C_{\rm gs_opt} &= \frac{C_{\rm gs1}\times P_{\rm opt}+C_{\rm gs2}}{P_{\rm opt}+C_{\rm gs2}} \\
C_{\rm gd} &= \frac{C_{\rm gs0}\times C_{\rm gs_opt}}{\left(1-\dfrac{V_{\rm new}}{V_{bi}}\right)^{U}}\times K_0\times K_2+C_{\rm gd0}\times C_{\rm gd_opt}\times K_1 \\
C_{\rm gd_opt} &= C_{\rm gd1}\times P_{\rm opt}+1 \qquad (7)
\end{aligned}$$

where U is constant, and

$$\begin{aligned}
K_0 &= \frac{1}{2}\times\left[1+\frac{V_{\rm eff1}-V_T}{\sqrt{(V_{\rm eff1}-V_T)^2+(\delta)^2}}\right] \\
K_1 &= \frac{1}{2}\times\left[1+\frac{V_{\rm gs}-V_{\rm gd}}{\sqrt{(V_{\rm gs}-V_{\rm gd})^2+(1/\alpha)^2}}\right] \\
K_2 &= \frac{1}{2}\times\left[1-\frac{V_{\rm gs}-V_{\rm gd}}{\sqrt{(V_{\rm gs}-V_{\rm gd})^2+(1/\alpha)^2}}\right] \\
V_{\rm eff1} &= \tfrac{1}{2}\times\left[V_{\rm gs}+V_{\rm gd}+\sqrt{(V_{\rm gs}-V_{\rm gd})^2+\Delta^2}\right] \\
V_{\rm eff2} &= \tfrac{1}{2}\times\left[V_{\rm gs}+V_{\rm gd}-\sqrt{(V_{\rm gs}-V_{\rm gd})^2+\Delta^2}\right] \\
V_{\rm new} &= \frac{1}{2}\times\left[V_{\rm eff1}+V_T+\sqrt{(V_{\rm eff1}-V_T)^2+\delta^2}\right] \qquad (8)
\end{aligned}$$

where δ and Δ are constant. Notation was basically in accordance with [11]. $P_{\rm opt}$ in these equations denotes the illumination-intensity parameter.

Since the output power of the laser diode of $\lambda = 635$ nm with 1 mW was not sufficient for examination of the illumination intensity dependence, more output power from the laser must be used for more accurate formulation for the future experiment. Using these equations, the computed $I_{\rm ds}$–$V_{\rm ds}$ curve and S-parameters were compared with the experimental data, as shown in Figs. 11 and 12. Agreement between them was found to be quite good.

Generally speaking, when the FET model has many elements in the equivalent circuit and many fitting parameters in the characteristic equation, good convergence cannot be obtained or it takes a very long time to extract the model parameters for a wide band. Even if the parameter extraction is achieved, it is hard to find out which value is reasonable and desired since there are many minimum points within the investigated range with respect to a function with many variables.

The most important thing for the parameter extraction using the simulator is how reliably initial values are given or how close the given initial values are to the final value. In order to obtain good convergence and the reliable parameters, the parameter extraction should be divided into several consecutive steps. A basic idea for this method is that the model should start from a simple one and be modified into a complex one, and the characteristic equation must have less unknowns and/or less fitting parameters and exchange them into the equation with many unknowns. In this procedure, it should be noted that the extracted values in the former step must be utilized as the initial values to the next step.

The concrete steps for this procedure used in this paper are described below.

1) The Y-parameters from the measured small-signal S-parameters were compared with the Y-parameters

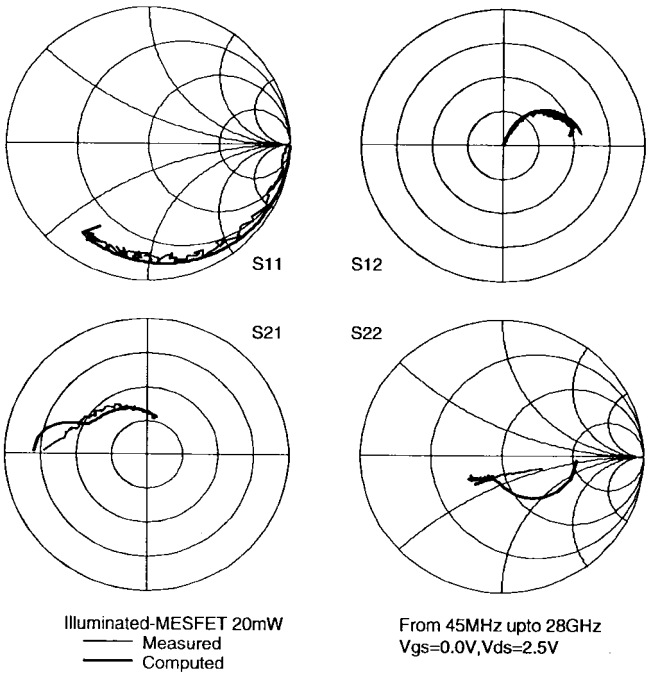

(a)

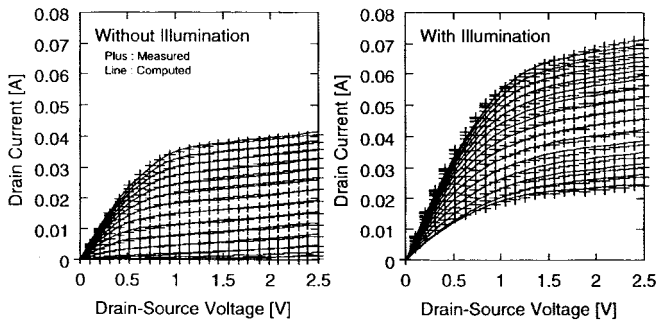

(b)

Fig. 11. Comparison between measured and computed data of dc and RF characteristics of illuminated MESFET.

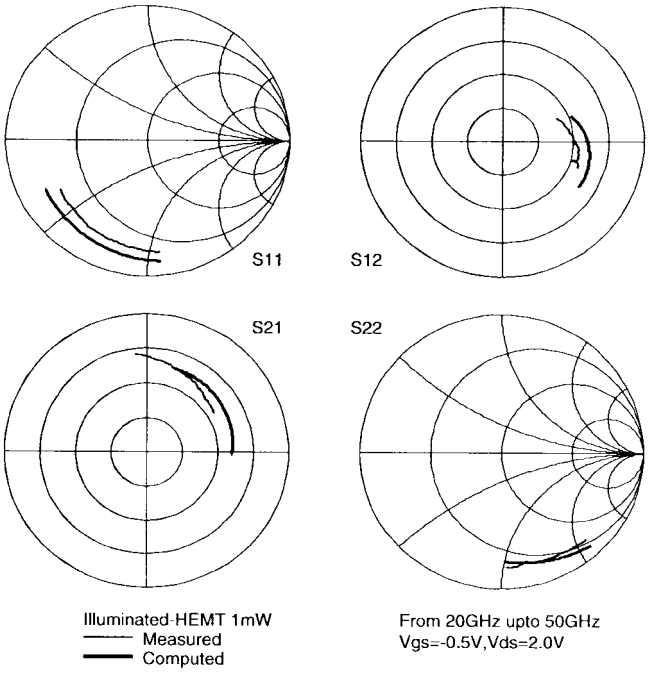

(a)

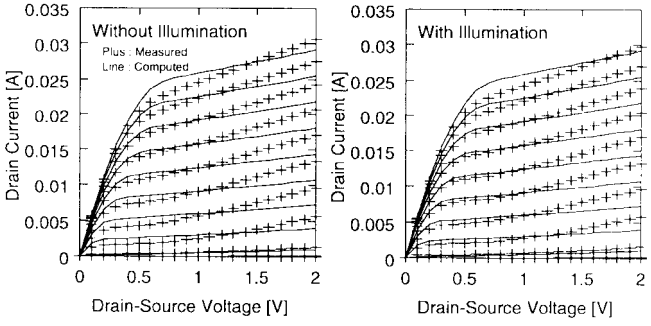

(b)

Fig. 12. Comparison between measured and computed data of dc and RF characteristics of illuminated HEMT.

with respect to the analyzed region in Fig. 6, and the six FET model parameters such as $C_{\rm gs}, R_{\rm in}$, etc., were extracted (Initial-Value 1 in Table I).

2) From observation, the typical FET model was modified for the frequency characteristics from the equivalent-circuit model to meet with those from the measured data in comparison with the Y-parameters, and then the parameter extraction using values of Initial-Value 1 was carried out again (the modified model/Initial-Value 2).
3) Utilizing the modified model and the Initial-Value 2 indicated in 2), with the Y-parameters from the measured S-parameters of the illuminated FET, the desired model to meet with the frequency characteristics from the measured data was obtained (the small-signal illuminated FET).
4) Utilizing the modified model and Initial-Value 2 indicated in 2) with the measured I–V characteristics of the FET without illumination, the fitting parameters of a nonlinear equation for $I_{\rm ds}$ such as the Curtice Cubic model and Statz model (used in this paper) were extracted (Initial-Value 3).
5) In order to describe the I–V characteristics as accurately as possible, the modified Statz model was applied as the second nonlinear equation for $I_{\rm ds}$. The fitting parameters in this nonlinear equation were then extracted using the measured I–V characteristics of the FET without illumination and Initial-Value 3 (Initial-Value 4).
6) Utilizing the modified Statz model and Initial-Value 4 indicated in 5), with the measured I–V characteristics of the illuminated FET, the model parameters and the fitting parameters of a nonlinear equation for $I_{\rm ds}$ including an illumination intensity parameter were extracted (the nonlinear $I_{\rm ds}$ equation for the illuminated FET).
7) Making use of the small-signal illuminated FET and the extracted parameters described in 3), the model parameters, and the nonlinear $I_{\rm ds}$ equation for the illuminated FET and the fitting parameters described in 6), the model parameters and the fitting parameters of the nonlinear

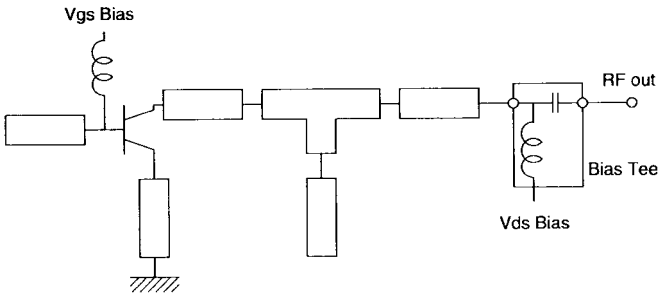

Fig. 13. Structure of MESFET oscillator.

capacitance such as C_{gs} and C_{dg} were determined with the measured S-parameters with the various applied dc voltages of V_{gs} and V_{ds} (the large-signal illuminated FET model in Fig. 9/the extracted parameters in Table II).

The measured S-parameters data used here were 400 points from 45 MHz to 50 GHz with the constant V_{gs} and V_{ds} and 90 sets with different V_{gs} and V_{ds}. Further, the measured data of 231 points from the I–V characteristics were used as 21 points from different V_{ds} with the constant V_{gs} and 11 sets with different V_{gs}. Using the technique described above, the good convergence and the reliable parameters can be relatively extracted.

IV. Optically Controlled Oscillator

Once the FET model including the illumination-intensity parameter is obtained, it can be applied to design the photonic microwave integrated circuit (the photonic MIC). Therefore, the proposed models were used in the simulator to design and analyze microwave and millimeter-wave optically controlled oscillators. The optically controlled MESFET oscillator has a series feedback loop and was fabricated on an alumina substrate ($\varepsilon r = 10$, thickness $= 0.635$ mm), while the HEMT oscillator was made in MMIC fashion with a buffer amplifier on an InP semi-insulating semiconductor substrate using a coplanar waveguide.

In the case of the MESFET oscillator, the negative resistance was set with $-50\ \Omega$ at 10 GHz using small-signal S-parameters. Configuration of this oscillator is shown in Fig. 13. In order to predict the steady-state oscillation frequency, a large-signal simulation was carried out with $V_{ds} = 2.5$ V and $V_{gs} = 0$ V. The predicted frequency was 10.7 GHz.

In the HEMT oscillator case, the operating frequency was designed at 37.5 GHz with $-40\ \Omega$ by using the measured small-signal S-parameters. The configuration and a photograph of the HEMT MMIC are shown in Fig. 14. In order to obtain the high power, a buffer amplifier was added to the output of the HEMT oscillator. Although a trial was made to predict the steady-state operating frequency using the harmonic-balance and the proposed FET model in the simulator under the structure condition described in Fig. 14, the reasonable operating frequency was not obtained due to a convergence problem of the simulation. This is because there are two nonlinear HEMT's (the oscillator HEMT and the buffer-amplifier HEMT) embedded in the MMIC to calculate. Instead, the start-up frequency was calculated under the two-

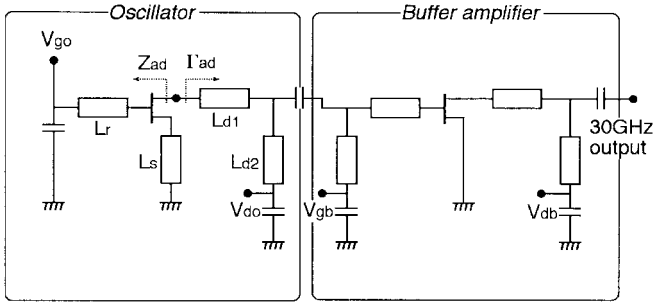

(a)

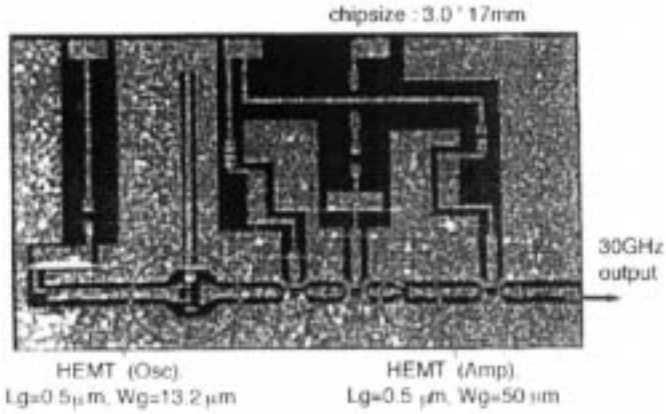

(b)

Fig. 14. Structure of HEMT MMIC oscillator.

HEMT condition shown in Fig. 14. In this case, using the proposed nonlinear illuminated FET model under the condition settled with $V_{ds} = 2.5$ V, $V_{gs} = 0$ V, and $P_{opt} = 0$ for both HEMT's, the start-up frequency of 31.1 GHz was obtained. This difference between the design frequency by the measured data and the simulated one from the model may result from an error from the nonlinear device modeling at the higher frequency.

Based on the design concept above, an optically controlled microwave hybrid integrated circuit (HIC) oscillator with the GaAs MESFET was fabricated. The operation frequency of the optically controlled MESFET oscillator was 10.3 GHz with $V_{ds} = 2.5$ V, $I_{ds} = 26$ mA, and $V_{gs} = 0$ V. The measured RF output was 5.50 dBm. In addition, a millimeter-wave MMIC oscillator with an InP HEMT was also made. This HEMT MMIC operated at 34.8 GHz with $V_{ds} = 2.5$ V, $I_{ds} = 20$ mA (including the buffer amplifier), and $V_{gs} = 0$ V, and its output power was 3 dBm.

The measured optical tuning ranges by the laser diode with 635 nm and 1 mW were plotted in Fig. 15 in comparison with the electrical tuning ranges with respect to V_{gs} with the constant V_{ds} without illumination. Since the spot diameter (about 8 mm) was relatively large, illumination covered the whole chip of the MMIC; hence, all HEMT's and other elements were lighted. Therefore, the operation of the buffer amplifier as well as a resistor may also be affected by the illumination, and then, the operation frequency shift will occur at the zero gate-bias voltage. From this consideration, it may

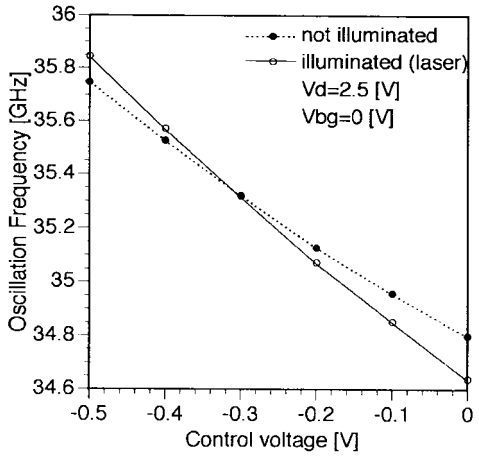

Fig. 15. Optical tuning range of HEMT MMIC oscillator.

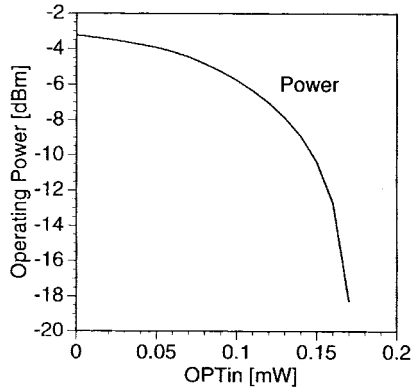

Fig. 16. Computed output power of optically controlled MESFET oscillator.

be possible that the maximum increasing optical tuning range of about 300 MHz at $V_{\rm gs} = -0.5$ V is obtained in the case where only the oscillator HEMT is illuminated.

The computed output power of the MESFET oscillator under illumination is shown in Fig. 16. From the observation of the simulation results, it appeared that the oscillation frequency and the output power decreased as illumination intensity increased. This effect resulted from the variation of the drain–source capacitance of $C_{\rm ds}$, $R_{\rm opt}$, and $C_{\rm opt}$. Particularly, the variation on $C_{\rm ds}$ resulted in the optical operating frequency shift of the oscillator under illumination. The variation of $R_{\rm opt}$ and $C_{\rm opt}$ caused the decrease in gain of the FET; hence, the output power was decreased by the illumination.

The investigation of the illumination effect on the HEMT MMIC using the proposed FET model in the simulator was attempted. However, since the convergence problem in the harmonic-balance simulation still occurred under the illumination condition, it is not possible to compare the calculated frequencies using the proposed model with the experimental data. Instead, in order to confirm validity of the illuminated FET model, the simulated start-up frequencies using the illuminated FET model and the measured small-signal S-parameters of the HEMT were compared. Table III shows the calculation results for both the dark and illumination cases. In both cases, the tendency of increasing the operating frequency can be seen,

TABLE III
COMPARISON OF THE START-UP FREQUENCY BETWEEN THE MODEL AND THE MEASUREMENT

	Gate Voltage [V]	start-up Frequency [GHz]	
		Model	Measurement
Dark	0.00	33.06	33.10
	-0.50	33.08	33.32
Illuminated	0.00	32.81	33.30
	-0.50	32.93	33.12

and agreement between them looks good. From observation of these data, it is believed that the proposed FET model with the illumination-intensity parameter is useful for the simulation of the photonic MMIC.

Thus far, only the simple illuminated FET model without consideration of the area of illumination in the FET gate periphery was discussed. In order to accurately simulate the experimental illumination status for the measurement of the FET, the hybrid model was investigated for the illuminated FET, taking into account the illuminated area as a fraction of the total gate periphery. The hybrid model consisted of the illuminated model and the normal model with the ratio of the illuminated area to the nonilluminated area.

As expected, the values of the model parameter including the illumination-intensity parameter approximately increased according to the area ratio. Using this model, the FET characteristics were able to be explained with acceptable agreement with the experimental data. However, there is no way to investigate such extreme phenomena inside the FET. Further, the convergence for the operation frequency of the optically controlled oscillator in both cases was not obtained under use of the harmonic-balance analysis. This may result from the fact that too many nonlinear parameters were involved in the simulation and that the model parameters including the illumination-intensity parameter became too sensitive to converge for the oscillation frequency. It is one of future research items to find out how to obtain the operation frequency of the optically controlled oscillator taking account of the illumination area ratio using the harmonic balance in the simulator.

V. CONCLUSIONS

This paper described modeling of an illuminated GaAs MESFET and an InP HEMT. In addition, analysis and experimental results of optically controlled microwave and millimeter-wave HIC and MMIC oscillators were presented. Further simulation results and comparison with experimental data were reported for the optically controlled oscillator using the novel FET model including an illumination-intensity parameter. The illumination effect on the oscillators can be described well in the harmonic-balance simulation with good agreement. Therefore, the proposed FET model is very effective and useful for the design of a photonic MMIC operated at a millimeter-wave frequency.

ACKNOWLEDGMENT

The authors thank the students of author Kawasaki's laboratory, Tokai University, Kanagawa, Japan, for their assistance.

The authors also thank Dr. K. Hara, T. Taguchi, and Y. Ueno, DENSO Research Laboratory, Aichi, Japan, for encouragement, and M. Yoneyama, Dr. T. Shibata, and E. Sano, NTT System Electronics Laboratory, Kanagawa, Japan, for useful suggestions.

REFERENCES

[1] A. J. Seeds, "Microwave opto-electronics: Principles, applications and future prospects," in *Proc. 24th European Microwave Conf.*, Cannes, France, Sept. 1994, pp. 8–22.

[2] Y. Soda, K. Tsukamoto, and S. Komaki, "Multichannel coherent SCM optical transmission system using radio-to-optic direct conversion scheme," in *MWP'96, Satellite Workshop, ATRI*, Kyoto, Japan, Dec. 1996, pp. 41–44.

[3] S. Kawasaki and T. Itoh, "Optical control of active integrated antennas using microwave-optical interaction," in *Electron. Commun. Japan*, vol. 78, no. 2, Jan. 1995, pp. 33–41.

[4] S. Kawasaki, M. Kimura, H. Shiomi, T. Wakabayashi, M. Funabashi, and K. Ohata, "Optical control of MMIC oscillators and model parameter analysis of an illuminated FET at the Ka- and V-band," in *IEEE MTT-S Int. Microwave Symp. Dig.*, Orlando, FL, May 1995, pp. 1287–1290.

[5] R. N. Simons, "Microwave performance of an optically controlled AlGaAs/GaAs high electron mobility transistor and GaAs MESFET," *IEEE Trans. Microwave Theory Tech.*, vol. MTT-35, pp. 1444–1455, Dec. 1987.

[6] A. Madjar, P. R. Herczfeld, and A. Paolella, "Analytical model for optically generated currents in GaAs MESFET's," *IEEE Trans. Microwave Theory Tech.*, vol. 40, pp. 1681–1691, Aug. 1992.

[7] D. Yang, P. Bhattacharya, R. Lai, T. Brock, and A. Paolella, "Optical control and injection locking of monolithically integrated $In_{0.53}Ga_{0.47}As/In_{0.52}Al_{0.48}As$ MODFET oscillators," *IEEE Trans. Electron Devices*, vol. 42, pp. 31–37, Jan. 1995.

[8] S. Kawasaki and T. Itoh, "Optical interaction of active integrated antennas," in *Proc. 24nd European Microwave Conf.*, Cannes, France, Sept. 1994, pp. 185–193.

[9] H. Shiomi, M. Yoneyama, T. Shibata, E. Sano, and S. Kawasaki, "A simple microwave optically controlled oscillator operating with optical signals designed by an illuminated FET model," in *MWP'96*, Kyoto, Japan, Dec. 1996, pp. 281–284.

[10] J. M. Golio, Ed., *Microwave MESFET's and HEMT's.* Norwood, MA: Artech House, 1991, ch. 2.

[11] J. Onomura, S. Watanabe, and S. Kamishima, "An accurate FET model for microwave nonlinear circuit simulation," *IEICE Trans. Electron.*, vol. E-78-C, no. 9, pp. 1223–1228, Sept. 1995.

Shigeo Kawasaki received the B.S. and M.S. degrees in electrical engineering from Waseda University, Tokyo, Japan, in 1979 and 1981, respectively, and the Ph.D. degree in electrical engineering from the University of California at Los Angeles (UCLA), in 1993.

In 1990, he was a Research Assistant at the University of Texas at Austin. From 1991 to 1993, he was a Graduate Student Researcher at UCLA. Since April 1994, he has been with Tokai University, Kanagawa, Japan, where he is a Professor in the Department of Communication Engineering. In 1997, he was a Visiting Scholar at UCLA. His research activities include quasi-optical components, active integrated antenna-array design and its optical control, and nonlinear active-device modeling for microwave simulators. He has published over 50 papers and holds several patents.

Dr. Kawasaki is a member of the Institute of Electronics, Information, and Communication Engineers (IEICE), Japan.

Hidehisa Shiomi received the B.E. and M.E. degrees in communication engineering from Tokai University, Kanagawa, Japan, in 1994 and 1996, respectively, and is currently working toward the Ph.D. degree.

Mr. Shiomi is a student member of the Institute of Electronics, Information, and Communication Engineers (IEICE), Japan.

Kazuoki Matsugatani received the B.S. and M.S. degrees in electronics engineering from Kyoto University, Kyoto, Japan, in 1987 and 1989, respectively.

In 1990, he joined the Research Laboratory, DENSO Corporation, Aichi, Japan, where he has been studying InP-based HEMT's and MMIC's.

Mr. Matsugatani is a member of the Institute of Electronics, Information, and Communication Engineers (IEICE), Japan.